Neuroscience Letters 781 (2022) 136658

Contents lists available at ScienceDirect

Neuroscience Letters

journal homepage: www.elsevier.com/locate/neulet

Temporal expression of Laminin-111 in the developing rat larynx

Ian F. Caplan [a], Ignacio Hernandez-Morato [a,*], Michael J. Pitman [a,b]

[a] Columbia University Irving Medical Center/New York Presbyterian, Department of Otolaryngology Head & Neck Surgery, New York, NY, USA
[b] Columbia University Irving Medical Center/New York Presbyterian, The Center for Voice and Swallowing, Department of Otolaryngology Head & Neck Surgery, New York, NY, USA

ARTICLE INFO

Keywords:
Laminin
Netrin-1
Recurrent laryngeal nerve
Embryo
Development
Vocal fold paralysis

ABSTRACT

Laminin-111 is a basement membrane protein that participates in motor innervation and reinnervation. During axonal pathfinding, laminin-111 interacts with netrin-1 (NTN1) and changes its attractant growth cone properties into repulsion. While previous models of recurrent laryngeal nerve (RLN) transection show increased Laminin-111 and NTN1 production after injury, developmental expression in the larynx has not been defined. This study investigates the expression of laminin-111 in laryngeal muscles during primary laryngeal innervation of Sprague Dawley rats. Adult larynges and embryos were sectioned for immunohistochemistry with βIII-Tubulin, laminin subunit α-1 (LAMA1), NTN1, and α-bungarotoxin. Sections were processed for single-molecule inexpensive RNA fluorescence *in situ* hybridization analysis of LAMA1 mRNA. LAMA1 expression increased in all intrinsic laryngeal muscles, except the medial thyroarytenoid (MTA), at E20.5. At E20.5 there was increased expression in the lateral thyroarytenoid (LTA) and posterior cricoarytenoid (PCA) compared to the MTA. NTN1 upregulation was limited to the LTA and lateral cricoarytenoid (LCA) at E16.5 without any increase in the MTA or PCA. LAMA1 and NTN1 expression did not strictly follow expected patterns relative to the known timing of innervation and does not appear to be acting similarly to its role following RLN injury. These differences between developmental and post-injury innervation provide targets for investigations of therapeutics after nerve injury.

1. Introduction

The larynx serves a critical role in phonation, airway protection, and respiration. The ability to accomplish all of these functions is facilitated by vocal fold movement, which is controlled by the intrinsic laryngeal muscles supplied by two branches of the vagus nerve. While there are anastomoses between the recurrent laryngeal nerve (RLN) and the superior laryngeal nerve (SLN), all intrinsic laryngeal muscles are primarily innervated by the RLN except for the cricothyroid (CT) muscles which receive predominantly SLN innervation [1]. The RLN is susceptible to injury during a multitude of surgical procedures and resulting vocal fold paralysis is permanent in roughly 1% of all thyroid and parathyroid surgeries and reported to be as high as 25% in some skull base surgeries [2–4]. This results in significant healthcare costs and patient morbity with dysphagia and dysphonia. Following severe RLN injury the distal nerve segment degenerates, resulting in laryngeal muscle denervation, and the proximal end undergoes spontaneous regeneration via axonal projections towards the original target [5,6]. However, functional regeneration is complicated by disorganized synkinetic motor axon reinnervation of the laryngeal muscles [7]. As a result of this non-selective reinnervation, functional restoration of vocal fold movement is never achieved [8–13].

The larynx is a well conserved organ making it suitable for comparative anatomy and physiology. Previous rodent studies of the larynx during development have described the sequence of both vocal fold epithelial differentiation and innervation of the intrinsic laryngeal muscles (Fig. 1) [14,15]. During rat development, the RLN approaches the larynx and then branches dorsally towards the posterior cricoarytenoid (PCA) at embryonic day (E)15.5. Ventral projections reach the lateral cricoarytenoid (LCA) and lateral thyroarytenoid (LTA) around

Abbreviations: αBTX, alpha-bungarotoxin; βIIIT, beta III tubulin; DCC, deleted colorectal carcinoma; LAMA1, laminin subunitα-1; LAMB1, laminin subunitβ-1; LAMC1, laminin subunitγ-1; LCA, lateral cricoarytenoid; LTA, lateral thyroarytenoid; MTA, medial thyroarytenoid; NMJ, neuromuscular junction; NTN1, netrin-1; PBS, phosphate buffered saline; PBST, 0.3% triton in phosphate buffered saline; PCA, posterior cricoarytenoid; RLN, recurrent laryngeal nerve; SLN, superior laryngeal nerve; smiFISH, fluorescence in situ hybridization; SSC, saline sodium citrate.

* Corresponding author at: Columbia University Irving Medical Center, Otolaryngology-Head and Neck Surgery, 180 Fort Washington Avenue, Rm 860 8th Floor. Harkness Pavilion, New York, NY 10032, USA.

E-mail addresses: ic2537@cuc.columbia.edu (I.F. Caplan), ih2302@cumc.columbia.edu (I. Hernandez-Morato), mp3517@cumc.columbia.edu (M.J. Pitman).

https://doi.org/10.1016/j.neulet.2022.136658
Received 1 September 2021; Received in revised form 8 April 2022; Accepted 22 April 2022
Available online 25 April 2022

E16.5/E17.5 and once synapses are formed the neuromuscular junctions (NMJ) mature until completion at E21.5 [16]. As observed in other systems, the innervation of the larynx may be directed by the expression of several proteins involved in axonal elongation and axonal guidance such as neurotrophic factors [17–19]. One of the proteins reported to participate in this regeneration is Netrin-1 (NTN1), a neurotrophic factor and member of the laminin superfamily [20,21]. In addition to its role in CNS formation, NTN1 and its receptors play a critical role during innervation of the periphery and reinnervation after acute injury [22–25]. Interestingly, NTN1 and one of its receptors, deleted in colorectal carcinoma (DCC), demonstrate bifunctional attractive and repulsive action in growth cone dynamics according to the expression of

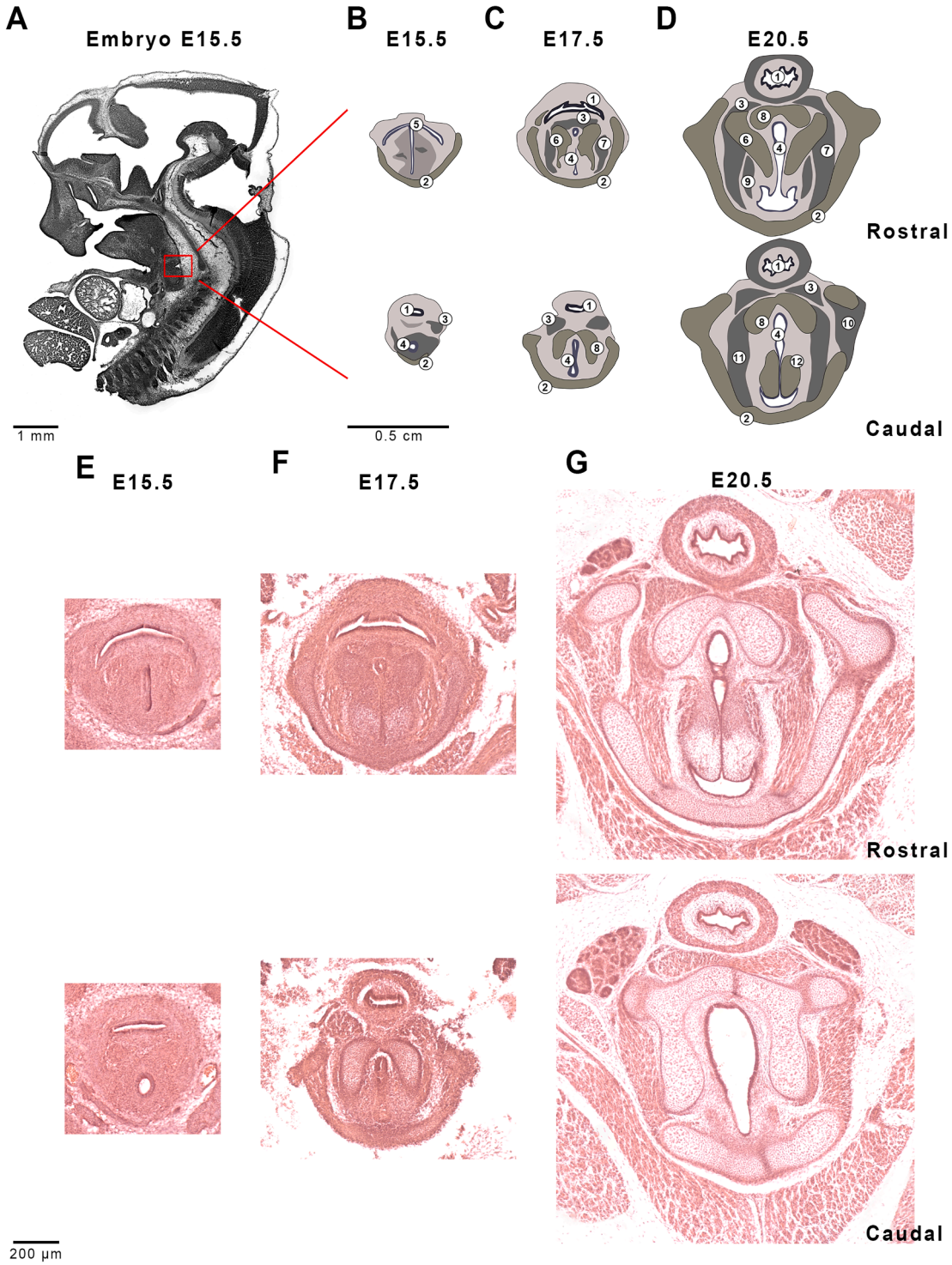

Fig. 1. Anatomy of the developing rat larynx Location of the larynx is found rostral to the embryo thorax and anterior to the developing spinal column (A). Both illustrated views of the larynx (B, C, D) and hematoxylin and eosin stained larynxes (E, F, G) are shown. The represented developmental stages are E15.5 (B, E), E17.5 (C, F), and E20.5 (D, G). Constituent parts of the larynx are as follows: 1 – esophagus, 2 – thyroid cartilage, 3 – posterior cricoarytenoid muscle, 4 – airway lumen, 5 – laryngopharynx, 6 – arytenoid cartilage, 7 – lateral thyroarytenoid muscle, 8 – cricoid cartilage, 9 – medial thyroarytenoid muscle, 10 – cricothyroid muscle, 11 – lateral cricoarytenoid muscle, 12 –vocal fold.

uncoordinated-5 or the presence of laminins in the environment surrounding the growth cone [26–29]. One laminin, laminin-111 identified by its subunit α-1 (LAMA1), plays an integral role in the embryonic basement membrane formation and functions as an axonal guidance cue [29–31]. Laminin-111 has also been shown to interact with the NTN1/DCC complex and convert NTN1 attraction to repulsion in retinal, vagal sensory, and trochlear neurons [32–34]. In the rat larynx, soon after RLN injury, NTN1 and LAMA1 are both upregulated showing differential temporal expression in laryngeal muscles which may influence axonal guidance during laryngeal muscle reinnervation [35].

Increased LAMA1 expression after RLN injury and its known interaction with NTN1 suggests laminin-111 may play a role in the reinnervation of the larynx. However, guidance cues expressed after RLN injury result in RLN axons being misguided and laryngeal muscles are reinnervated synkinetically. Therefore, in order to better understand the mechanism of reinnervation, we aim to investigate the correlation between LAMA1 and NTN1 expression during successful primary innervation of the abductor and adductor muscles of the rat larynx. Knowledge regarding differences between axon guidance during functional primary innervation of the larynx compared to synkinetic reinnervation may provide targets for investigation of future therapeutic intervention after nerve injury.

2. Materials and methods

2.1. Experimental animals

A total of six pregnant female Sprague Dawley rats were euthanized by intraperitoneal injection of 100 mg/kg ketamine with 10 mg/kg xylazine when litters reached E15.5, E16.5, E17.5, E18.5, E20.5, and E22.5. This study was conducted in accordance with the Public Health Service Policy on Humane Care and Use of Laboratory Animals, the National Institutes of Health Guide for the Care and Use of Laboratory Animals, and the Animal Welfare Act (7 U.S.C. et seq.). The Institutional Animal Care and Use Committee of Columbia University Medical Center approved the animal use protocol.

2.2. Tissue preparation

Pregnant female rats underwent transcardiac perfusion with 0.9% normal saline followed by 4% paraformaldehyde in phosphate buffered saline (PBS). Adult larynges and full embryos were postfixed in 4% paraformaldehyde in PBS overnight at 4 ℃, then 15% sucrose in PBS overnight and then 30% sucrose in PBS. Embryos were truncated at the thorax and the superior halves were embedded in optimal cutting temperature compound before sectioning at 14 μm on gelatin coated glass slides for immunohistochemistry and at 10 μm on glass slides for single molecule inexpensive RNA fluorescence *in situ* hybridization (*smiFISH)*.

2.3. Immunohistochemistry

Four embryos were used for each developmental age (n = 4). Sections were washed in PBS then incubated at 4 ℃ with 0.3% Triton in PBS (PBST). Slides prepared for NTN1 were additionally post-fixed in 4% PFA for 10 min and heat treated at 60 ℃ in 1x citrate buffer, before blocking at room temperature with 1% bovine serum albumin and 0.02% PBST followed by incubation in the appropriate primary antibody overnight. Secondary antibodies were applied before mounting with Fluoromount aqueous mounting medium (Sigma-Aldrich, St. Louis, Missouri). A full list of antibodies can be found in Table S1.

All 16 images of each laryngeal muscle were acquired with a fluorescent microscope on day of staining with standardized exposure time. These images were used for ImageJ analysis with threshold chosen by the investigators to minimize background signal. Fluorescence was measured by mean gray value (MGV), defined as the sum of gray values divided by the total number of pixels in the selection, and subsequently converted to mean pixel intensity [36]. These results are reported as optical density (OD) estimated by, OD = log10(255/mean pixel intensity), for standardization of fluorophore concentration [37,38]. All OD measurements were normalized to adult LTA or cerebellum, for LAMA1 and NTN1, respectively.

Specific attention to E20.5 data was taken due to a uniform increase in MGV following use of a new lot of LAMA1 primary antibody. Existing E16.5 and E22.5 embryos demonstrated 82.4% of the fluorescent intensity compared to age-matched experiments with the new antibody. Presented E20.5 data has been corrected by this figure.

2.4. Probes

In situ hybridization probes were designed using the open source Oligostan program as per Tsanov et al [39]. We utilized this coding package using R studio version 4.0.2 to generate probes to the rat LAMA1 coding transcript [40]. 24 probes were selected and conjugated to the Flap-X sequence in a dry 96-well plate as well as the secondary Flap-X probes conjugated to digoxigenin (IDT, Coralville, Iowa).

2.5. smiFISH and quantification

Two embryos (n = 2) with a minimum of two images per muscle were used for analysis. Procedure for *smiFISH* immunostaining was performed as described by Tsanov *et al.* with the following modifications [39]. Sections were washed twice at room temperature for 5 min in PBS, followed by 20 min in PBST, and finally 20 min in 15% formamide in 1x saline sodium citrate (SSC). Slides were then incubated overnight at 37 ℃ in hybridization mixture, washed twice for 30 min at 37 ℃ in 15% formamide in SSC, and then 10 min in PBST at room temperature. Secondary antibody was applied and slides were covered using Vectashield antifade mounting medium with DAPI (H-1200, Vector Laboratories).

3D image acquisition was performed at 40x with a Zeiss LSM confocal microscope. Z-stacks were deconvolved using ImageJ and associated plugins, specifically DeconvolutionLab2 and PSF generator [41]. Stacks were transformed to maximum 2D projections for final counting. Two independent observers were blinded for puncta quantification. Mean puncta for negative controls were subtracted from each count for normalization.

2.6. Statistical analysis

Comparison of means between multiple groups was performed using two-way ANOVA with Tukey's post-hoc test to assess differences between two means. A $p < 0.05$ was considered statistically significant. Statistics were performed using Python and associated statistical packages [42]. See the associated python files in the data repository for stepwise annotation of the raw fluorescent intensity analysis [43].

3. Results

3.1. Laminin-111 subunit colocalization

We sought to ensure that the expression of laminin-111 could be reliably detected in the intrinsic laryngeal muscles. Expression for all three laminin subunits was seen uniformly in the adult larynx and localized to the basal lamina surrounding each muscle fiber. Colocalization was found between LAMA1/LAMB1 in the LTA (Fig S1 A-C) and PCA (Fig S1 G-I), as well as between LAMA1/LAMC1 in the LTA (Fig S1 D-F) and PCA (Fig S1 J-L). No staining was observed in the cytoplasm of the muscle fibers in adult animals.

3.2. NMJ formation and muscle maturation

The progression of laryngeal development was qualitatively and

quantitatively assessed by examining NMJ formation with αBTX and RLN innervation with βIIIT. At E15.5 both the PCA and LCA showed βIIIT penetration (Fig. 2 A-B) and early consolidation of αBTX (Fig S2 B). First signs of LTA innervation and concurrent αBTX consolidation can be seen at E17.5 (Fig. 2I, Fig S2 B). By E18.5 the medial thyroarytenoid (MTA) began to mature with evidence of NMJ formation (Fig S2 B).

There was unchanged αBTX OD from E15.5-E18.5 in the PCA. Similarly, αBTX in the LCA was unchanged from E15.5 through E17.5. The first significant increase in αBTX OD occurred at E17.5 in the LTA (0.55 ± 0.03 vs. 0.69 ± 0.09, $p = 0.001$). MTA showed significant muscle maturation and increased NMJ intensity between E18.5 and E20.5 (0.63 ± 0.08 vs. 0.76 ± 0.06, $p = 0.001$). All muscles, except for the PCA, demonstrated increased αBTX OD between E20.5 and E22.5 as embryos approached full maturation.

3.3. Temporaspatial changes in protein expression

Analysis of LAMA1 expression showed an increase in expression from E15.5 to E22.5 in all muscles identified (Fig. 3A). LAMA1 was expressed at a consistently low level from E15.5 through E17.5 In the PCA, LCA, and CT (Fig. 3B). The LTA was the sole muscle which demonstrated a significant increase in expression at E17.5 compared to E15.5 (0.93 ± 0.06 vs. 0.84 ± 0.05, $p = 0.003$). Beginning at E18.5 there was a significant increase in LAMA1 expression compared to the E15.5 baseline in the PCA ($p < 0.001$) and CT ($p = 0.003$), however, LCA expression remained consistent from E15.5 to E18.5. The MTA is unique in that LAMA1 expression becomes reliably measurable only at E18.5 (Fig. 3B). There was a significant increase in LAMA1 in the MTA from E20.5 to E22.5 (0.93 ± 0.05 vs. 1.01 ± 0.08, $p = 0.047$). For all other intrinsic muscles there was slight, but not significant, changes in LAMA1 expression between E20.5 and E22.5 where mean normalized OD ranged from 0.93 to 1.04.

NTN1 expression in the LTA was greater at E16.5 when compared to all other embryonic ages (Fig. 4A). Similarly, E16.5 expression in the LCA was greater than all other ages except E18.5 (1.21 ± 0.33 vs. 1.01 ± 0.30, $p = 0.114$). However, there was no difference in NTN1 expression across development in the MTA ($p = 0.122$), PCA ($p = 0.056$), or CT ($p = 0.098$).

NTN1 expression was only different between muscles at E16.5 ($p = 0.032$), with LTA expression being the greatest. LAMA1 expression was significantly increased in the LTA compared to the PCA at E17.5 ($p = 0.006$). And at E20.5 the MTA had decreased expression when compared to the PCA ($p < 0.001$) and the LTA ($p < 0.001$). All muscles showed comparable intensity at E15.5, E16.5, E18.5, and E22.5 (Table 1).

3.4. smiFISH measurement of LAMA1 mRNA expression

LAMA1 mRNA expression was relatively stable across every age

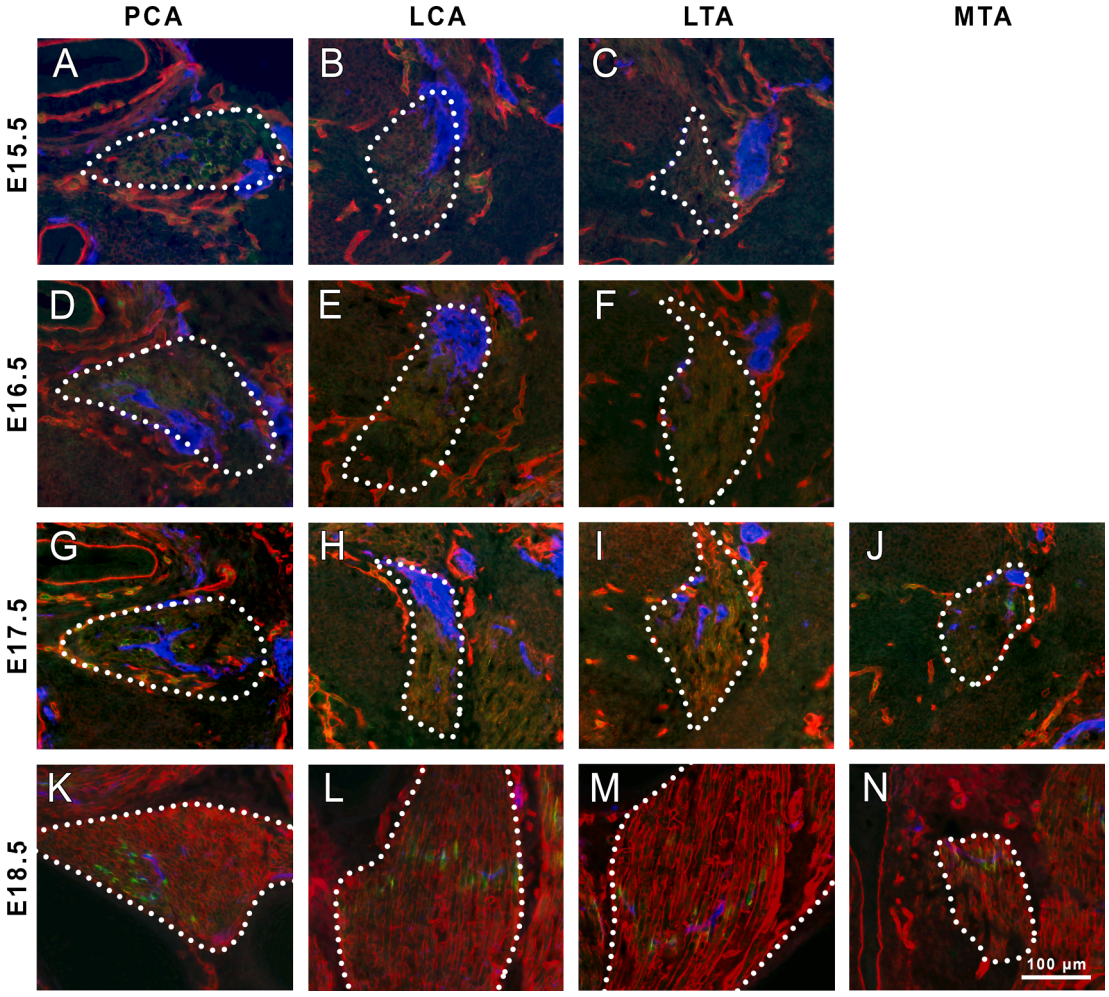

Fig. 2. Embryonic laryngeal maturation and innervation. E15.5 (A-C) shows innervation of both PCA and LCA with early NMJ formation. There is continued innervation and αBTX consolidation at E16.5 (D-F) in the PCA and LCA. First evidence of LTA innervation occurs at E17.5 (I) as well as very early signs of MTA formation (J). By E18.5 (K-N) all four muscles demonstrate localized NMJ's with local innervation. All muscles are oriented posterior to anterior on the left side of the larynx. Dashed lines define border of the muscle indicated in each column. Bar indicates 100 μm. LAMA1 (red); αBTX (green); βIIIT (blue).

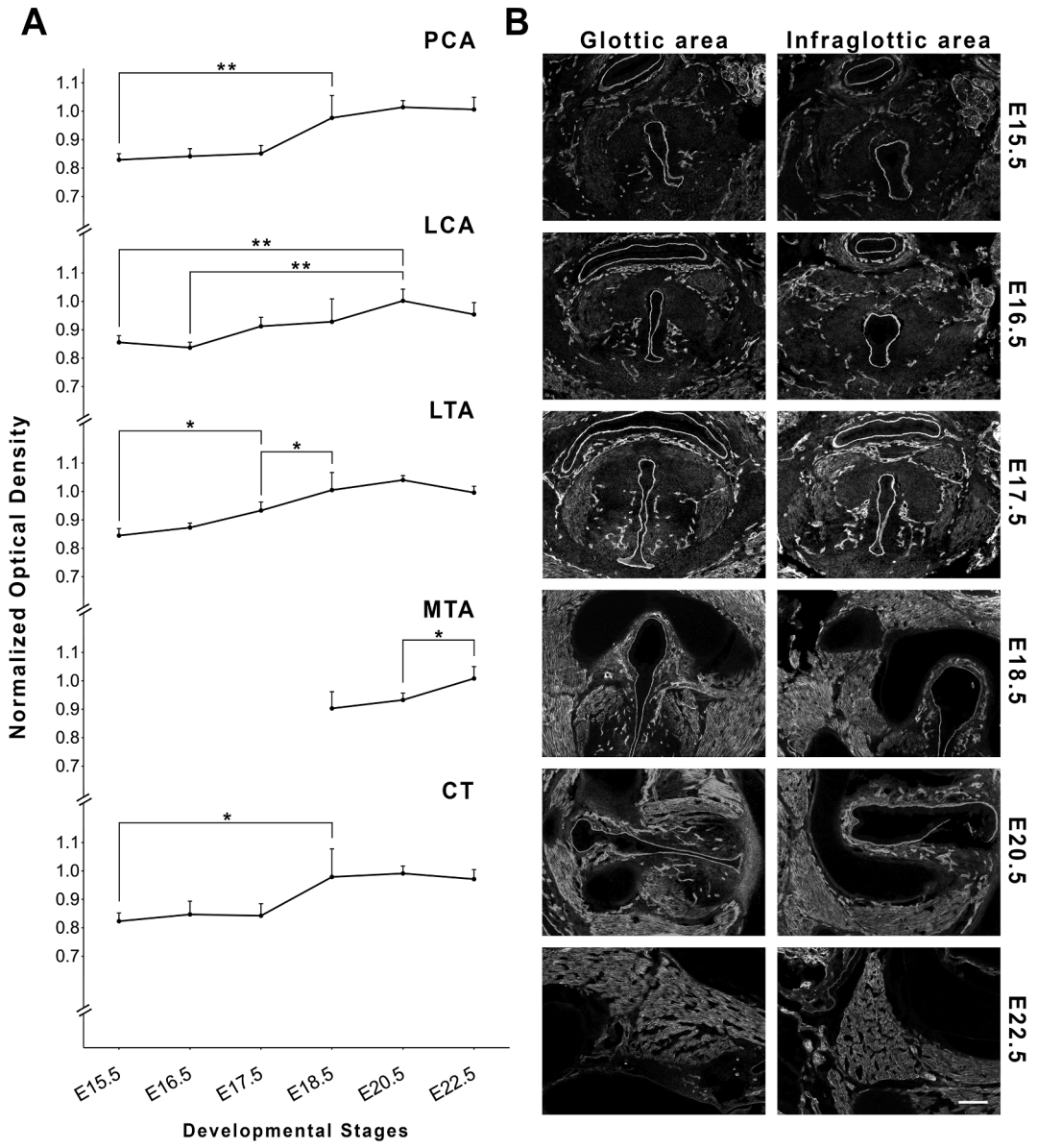

Fig. 3. Quantification of LAMA1 IHC expression. Expression of LAMA1 was quantified across the developmental timepoints (A). Normalized baseline OD at E15.5 was: PCA = 0.83 ± 0.04, LCA = 0.86 ± 0.05, LTA = 0.84 ± 0.05, CT = 0.82 ± 0.06. When compared to baseline expression in each muscle, significant increase in expression was seen at E17.5 in the LTA (0.93 ± 0.06, $p = 0.003$), at E18.5 in the PCA (0.98 ± 0.16, $p < 0.001$) and CT (0.980.20, $p = 0.003$), and lastly the LCA at E20.5 (1.00 ± 0.08, $p < 0.001$). There was no further increase in LAMA1 up to E22.5 except from E20.5 to E22.5 in the MTA (0.93 ± 0.05 vs 1.01 ± 0.08, $p = 0.047$). Representative 10x images demonstrate LAMA1 expression patterns throughout development (B). * $p < 0.05$ and ** $p < 0.001$.

studied (Table 2). There was a significant increase in the PCA at E18.5 compared to E15.5 ($p = 0.034$). There was no other significant change in mRNA expression identified (Fig S3).

4. Discussion

Laminins are integral basement membrane proteins forming heterotrimers required for even the earliest embryonic implantation and development [30]. These proteins also act as attractant signals both for in vitro axonal guidance as well as during peripheral nerve regeneration [29,31,44–46]. NTN1, a laminin superfamily member, is involved in nervous system development and exhibits bidirectional growth cone activity depending on the receptors encountered in its local environment [20,21,23,26,27,30,47]. Our previous work demonstrated an increase in LAMA1 and NTN1 expression following rat RLN injury that was chronologically coordinated with nerve reinnervation suggesting a repulsive role for NTN1 after synapse formation [32,34,35]. While this reinnervation leads to synkinetic, nonfunctional reinnervation, understanding the differences in embryonic innervation may elucidate targets for therapeutic intervention [3,7–9].

This study demonstrated the expression pattern of laminin-111 and NTN1 in the developing rat larynx for the first time. Confirmation of developmental innervation patterns was done with quantification of αBTX OD for NMJ maturation at expected timing of innervation. Both the PCA and LCA received RLN innervation at E15.5 (Fig. 2) which correlates to the stable OD through E17.5. Increased αBTX OD in the LTA at E17.5 also correlates with observed innervation at this timepoint. Lastly the MTA received innervation at E18.5 and significant NMJ consolidation between E18.5 and E20.5 (Fig S2).

Analysis of LAMA1 expression patterns showed a baseline expression of LAMA1 across the larynx from E15.5-E17.5 followed by upregulation at E18.5. At E22.5 near birth, LAMA1 expression was comparable to that of the adult rat larynx control. LAMA1 expression (Table 2) was comparable between all intrinsic muscles, including the CT, except in two

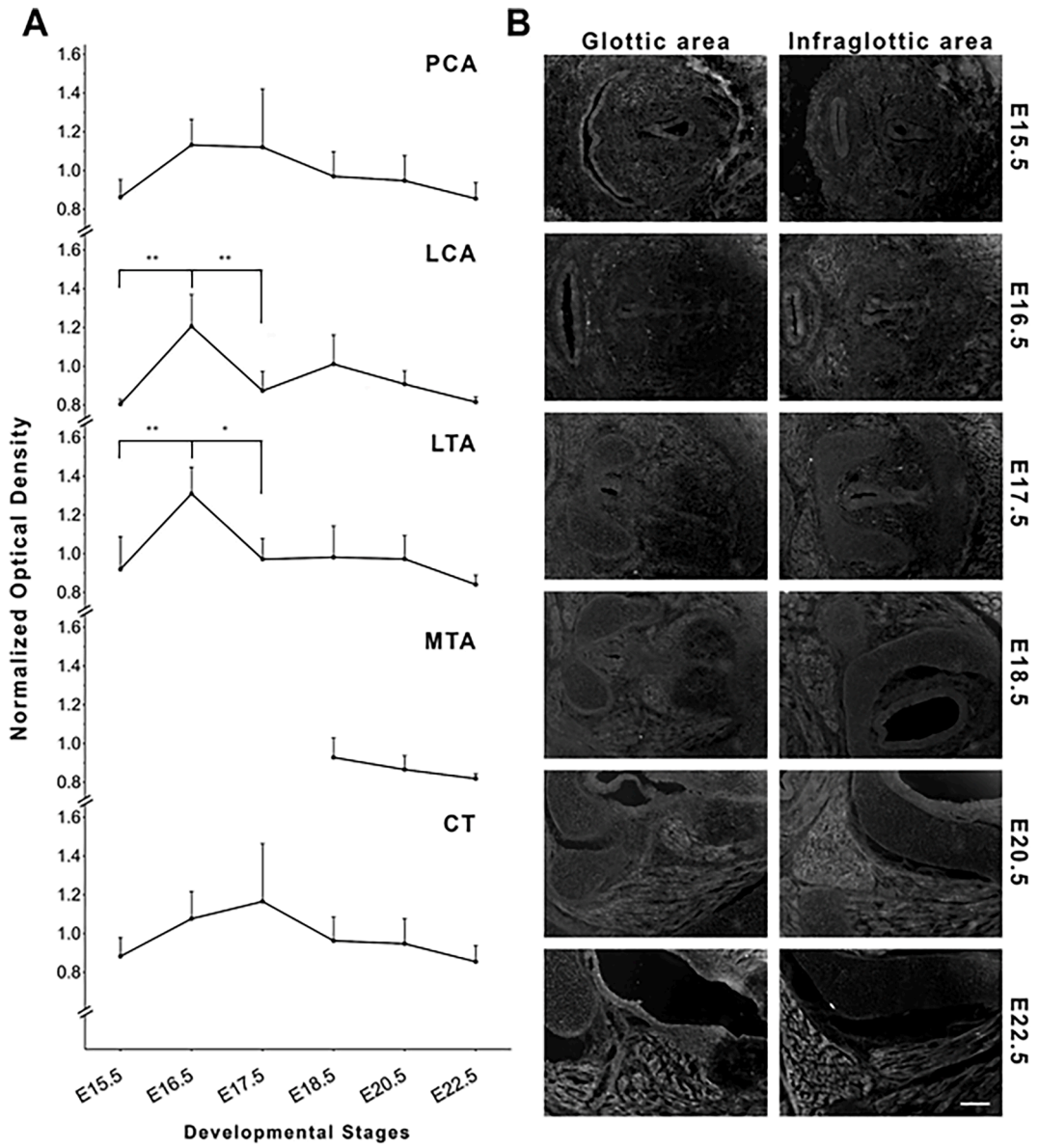

Fig. 4. Quantificaiton of NTN1 IHC Expression Expression of NTN1 was quantified across the developmental timepoints (A). Significant changes in OD were only found in the LCA and LTA. Elevated normalized OD in the LCA at E16.5 (1.21 ± 0.33) was greater than baseline E15.5 (0.80 ± 0.05, $p < 0.001$) and E17.5 (0.87 ± 0.20, $p < 0.001$). Elevated normalized OD in the LTA at E16.5 (0.92 ± 0.34) was greater than baseline E15.5 (0.92 ± 0.34, $p < 0.001$) and E17.5 (0.97 ± 0.21, $p = 0.005$). Representative 10x images demonstrate NTN1 expression patterns throughout development (B). * $p < 0.05$ and ** $p < 0.001$.

instances: There was intermuscle variation of LAMA1 expression where LTA expression was greater than the PCA at E17.5 and MTA less than that of the PCA and LTA at E20.5. As previously noted, laminin-111 activity is critical to basement membrane formation and the uniform increase in expression identified above is compatible with continuing maturation of the muscle fibers themselves rather than discrete upregulation at the time of initial innervation.

In comparison, NTN1 expression was notably elevated at E16.5 in the LTA and LCA, but there was no upregulation in the PCA nor in the MTA around the timing of expected innervation. In light of the comparable LAMA1 expression across the larynx, the proposed mechanism of NTN1/laminin-111 mediated repulsion requires that NTN1 expression be increased following innervation. But the data show isolated NTN1 upregulation at E16.5 in the LCA and LTA, and lack of further changes at E16.5 in the PCA, E18.5 in the LTA, or E20.5 in the MTA. Interestingly, LAMA1 expression was in fact lower in the MTA compared to the LTA at E20.5 while NTN1 was non-significantly elevated in the LTA compared to the MTA, which could correspond to the ultimate innervation of the MTA. However, with no other evidence of NTN1 upregulation the hypothesized temporal expression of these two trophic factors does not explain the pattern of primary laryngeal innervation.

It should also be noted that analysis of the *smiFISH* experiments was limited by a blinded two-observer method. The fluorescent intensity of the LAMA1 mRNA and background autofluorescence of the secondary antibody in negative controls were too similar for reliable automated differentiation (Sup. Fig. 3). Integrity was maintained by blinding the age and muscle of each image. The *smiFISH* results demonstrated that LAMA1 mRNA was detectable, however, there were no significant difference in the number of puncta identified across development. These results suggest that the increased expression of LAMA1 protein was not a result of increased mRNA transcription and it could therefore be a product of increased post-transcriptional events that were not assessed here.

Table 1
Trophic factor expression in laryngeal muscles at each developmental stage Values are reported as mean normalized optical density (OD) and standard deviation (SD). N/A indicates the muscle was not reliably identifiable at that embryonic age. * $p < 0.05$ and ** $p < 0.001$, † signifies value is also significantly different from LAMA1 OD of the LTA ($p < 0.001$).

		LAMA1			NTN1		
Age	Muscle	Normalized OD (SD)	p value	Tukey's Post Hoc	Normalized OD (SD)	p value	Tukey's Post Hoc
E15.5			0.294			0.512	
	PCA	0.83 (0.043)		Reference	0.86 (0.18)		Reference
	LCA	0.86 (0.048)		0.448	0.80 (0.050)		0.900
	LTA	0.84 (0.050)		0.785	0.92 (0.34)		0.900
	MTA	N/A		N/A	N/A		N/A
E16.5			0.285			0.032	
	PCA	0.85 (0.054)		Reference	1.13 (0.26)		Reference
	LCA	0.84 (0.038)		0.900	1.21 (0.33)		0.863
	LTA	0.87 (0.032)		0.437	1.31 (0.27)		0.270
	MTA	N/A		N/A	N/A		N/A
E17.5			<0.001			0.391	
	PCA	0.85 (0.056)		Reference	1.12 (0.60)		Reference
	LCA	0.91 (0.064)		0.061	0.87 (0.20)		0.399
	LTA	0.93 (0.061)		0.006*	0.97 (0.21)		0.770
	MTA	N/A		N/A	N/A		0.460
E18.5			0.351			0.775	
	PCA	1.03 (0.16)		Reference	0.97 (0.20)		Reference
	LCA	0.93 (0.16)		0.900	1.01 (0.30)		0.900
	LTA	1.01 (0.12)		0.900	0.98 (0.32)		0.900
	MTA	0.90 (0.12)		0.664	0.93 (0.20)		0.900
E20.5			<0.001			0.567	
	PCA	1.01 (0.047)		Reference	0.95 (0.26)		Reference
	LCA	1.00 (0.082)		0.900	0.91 (0.14)		0.900
	LTA	1.04 (0.031)		0.641	0.97 (0.24)		0.900
	MTA	0.93 (0.048)		< 0.001*†	0.87 (0.14)		0.780
E22.5			0.184			0.787	
	PCA	1.01 (0.086)		Reference	0.86 (0.17)		Reference
	LCA	0.95 (0.083)		0.290	0.82 (0.050)		0.800
	LTA	1.00 (0.045)		0.900	0.84 (0.10)		0.900
	MTA	1.01 (0.083)		0.900	0.82 (0.05)		0.851

Table 2
Assessment of temporal changes in LAMA1 mRNA expression in the intrinsic laryngeal musculature. Values are reported as mean puncta quantified and standard deviation (SD). of N/A indicates puncta were not reliably identifiable at that embryonic age. * $p < 0.05$ and ** $p < 0.001$.

Muscle	Age	Puncta (SD)	p value	Tukey's Post Hoc
LTA			0.871	
	E15.5	4.83 (5.62)		Reference
	E18.5	3.33 (2.95)		0.900
	E20.5	5.19 (2.51)		0.900
	E22.5	4.54 (4.12)		0.900
MTA			0.131	
	E15.5	N/A		N/A
	E18.5	12.65 (13.71)		Reference
	E20.5	3.18 (3.06)		0.136
	E22.5	3.08 (2.74)		0.149
LCA			0.118	
	E15.5	1.25 (1.13)		Reference
	E18.5	7.22 (7.60)		0.144
	E20.5	3.32 (2.11)		0.874
	E22.5	1.86 (2.44)		0.900
PCA			0.051	
	E15.5	0.86 (1.41)		Reference
	E18.5	6.75 (5.89)		0.034*
	E20.5	5.39 (4.10)		0.192
	E22.5	3.00 (2.19)		0.734
CT			0.350	
	E15.5	4.0 (4.19)		Reference
	E18.5	15.25 (13.37)		0.843
	E20.5	7.00 (3.36)		0.900
	E22.5	25.75 (28.22)		0.369

5. Conclusion

Herein we investigated the role of LAMA1 and NTN1 in the developing rat larynx and found differential expression of LAMA1 at E20.5 with decreased MTA expression compared to the LTA and NTN1 upregulation was limited to the LTA and LCA at E16.5. There was also significant upregulation of LAMA1 expression by E18.5 in most intrinsic laryngeal muscles. The observed LAMA1 upregulation in both the abductor and adductors and isolated NTN1 upregulation at E16.5 was unexpected. The repulsive interaction between NTN1 and LAMA1 is not observed across primary laryngeal innervation and differs starkly from that observed during dysfunctional reinnervation after RLN injury. These differences present targets for future investigation of therapeutics after such injury.

6. Sources of Funding

This work was supported by the National Institutes of Health: 1R01DC018060-1.

CRediT authorship contribution statement

Ian F. Caplan: Conceptualization, Methodology, Software, Validation, Formal analysis, Investigation, Resources, Data curation, Writing – original draft, Visualization. **Ignacio Hernandez-Morato:** Conceptualization, Methodology, Validation, Formal analysis, Resources, Writing – review & editing, Visualization. **Michael J. Pitman:** Conceptualization, Methodology, Resources, Writing – review & editing, Supervision, Project administration, Funding acquisition.

Acknowledgements

We thank Dr. Theresa Swayne and Dr. Emilia L. Muntenau, of the Confocal and Specialized Microscopy Shared Resource at Columbia University Herbert Irving Comprehensive Cancer Center for their assistance in imaging hematoxylin and eosin preparations of the larynx. This work was supported by the National Institutes of Health

1R01DC018060-1.

Appendix A. Supplementary data

Supplementary data to this article can be found online at https://doi.org/10.1016/j.neulet.2022.136658.

References

[1] Susan Standring, Larynx, in: Gray's Anatomy, 2020: pp. 717–734.
[2] D. Myssiorek, Recurrent laryngeal nerve paralysis: anatomy and etiology, Otolaryngologic Clinics of North America. 37 (2004) 25–44, https://doi.org/10.1016/S0030-6665(03)00172-5.
[3] J.P. Noordzij, R.H. Ossoff, Anatomy and physiology of the larynx, Otolaryngologic Clinics of North America. 39 (2006) 1–10, https://doi.org/10.1016/j.otc.2005.10.004.
[4] G.-R. Joliat, V. Guarnero, N. Demartines, V. Schweizer, M. Matter, Recurrent laryngeal nerve injury after thyroid and parathyroid surgery: Incidence and postoperative evolution assessment, Medicine. 96 (2017), e6674, https://doi.org/10.1097/MD.0000000000006674.
[5] T. Gordon, Peripheral nerve regeneration and muscle reinnervation, International Journal of Molecular Sciences. 21 (2020) 1–24, https://doi.org/10.3390/ijms21228652.
[6] X. Navarro, M. Vivó, A. Valero-Cabré, Neural plasticity after peripheral nerve injury and regeneration, Progress in Neurobiology. 82 (2007) 163–201, https://doi.org/10.1016/j.pneurobio.2007.06.005.
[7] R.L. Crumley, Laryngeal synkinesis revisited, Annals of Otology, Rhinology and Laryngology. 109 (2000) 365–371, https://doi.org/10.1177/000348940010900405.
[8] P.W. Flint, D.H. Downs, M.D. Coltrera, Laryngeal synkinesis following reinnervation in the rat: Neuroanatomic and physiologic study using retrograde fluorescent tracers and electromyography, Annals of Otology, Rhinology & Laryngology. 100 (1991) 797–806, https://doi.org/10.1177/000348949110001003.
[9] B. Benjamin, Vocal cord paralysis, synkinesis and vocal fold motion impairment, ANZ Journal of Surgery. 73 (2003) 784–786, https://doi.org/10.1046/j.1445-2197.2003.02799.x.
[10] I. Hernández-Morato, F.J. Valderrama-Canales, G. Berdugo, G. Arias, S. Mchanwell, J. Sañudo, T. Vázquez, A. Pascual-Font, Reorganization of laryngeal motoneurons after crush injury in the recurrent laryngeal nerve of the rat, Journal of Anatomy. 222 (2013) 451–461, https://doi.org/10.1111/joa.12031.
[11] I. Hernández-Morato, G. Berdugo-Vega, J.R. Sañudo, S. Mchanwell, T. Vázquez, F. J. Valderrama-Canales, A. Pascual-Font, Somatotopic changes in the nucleus ambiguus after section and regeneration of the recurrent laryngeal nerve of the rat, Anatomical Record. 297 (2014) 955–963, https://doi.org/10.1002/ar.22877.
[12] M.J. Pitman, P. Weissbrod, R. Roark, S. Sharma, S.D. Schaefer, Electromyographic and histologic evolution of the recurrent laryngeal nerve from transection and anastomosis to mature reinnervation, Laryngoscope. 121 (2011) 325–331, https://doi.org/10.1002/lary.21290.
[13] I. Hernandez-Morato, S. Koss, S. Sharma, M.J. Pitman, Influence of Netrin-1 on reinnervation of laryngeal muscles following recurrent laryngeal nerve injury, Neuroscience Letters. 653 (2017) 244–249, https://doi.org/10.1016/j.neulet.2017.05.033.
[14] V. Lungova, J.M. Verheyden, J. Herriges, X. Sun, S.L. Thibeault, Ontogeny of the mouse vocal fold epithelium, Developmental Biology. 399 (2015) 263–282, https://doi.org/10.1016/J.YDBIO.2014.12.037.
[15] V. Lungova, J.M. Verheyden, X. Sun, S.L. Thibeault, β-Catenin signaling is essential for mammalian larynx recanalization and the establishment of vocal fold progenitor cells, Development. 145 (2018), https://doi.org/10.1242/DEV.157677.
[16] M.J. Pitman, C.E. Berzofsky, O. Alli, S. Sharma, Embryologic innervation of the rat laryngeal musculature - A model for investigation of recurrent laryngeal nerve reinnervation, Laryngoscope. 123 (2013) 3117–3126, https://doi.org/10.1002/lary.24216.
[17] D. Bonanomi, S.L. Pfaff, Motor Axon Pathfinding, Cold Spring Harbor Perspectives in Biology. 2 (2010) a001735–a001735. 10.1101/cshperspect.a001735.
[18] S. Guthrie, Patterning and axon guidance of cranial motor neurons, Nature Reviews Neuroscience. 8 (2007) 859–871, https://doi.org/10.1038/nrn2254.
[19] A. Varela-Echavarría, A. Tucker, A.W. Püschel, S. Guthrie, Motor Axon Subpopulations Respond Differentially to the Chemorepellents Netrin-1 and Semaphorin D, Neuron. 18 (1997) 193–207, https://doi.org/10.1016/S0896-6273(00)80261-5.
[20] K.L.W. Sun, J.P. Correia, T.E. Kennedy, Netrins: versatile extracellular cues with diverse functions, Development. 138 (2011) 2153–2169, https://doi.org/10.1242/dev.044529.
[21] S. Rajasekharan, T.E. Kennedy, The netrin protein family, Genome Biology. 10 (2009) 239, https://doi.org/10.1186/gb-2009-10-9-239.
[22] T.E. Kennedy, T. Serafini, JoséR. de la Torre, M. Tessier-Lavigne, Netrins are diffusible chemotropic factors for commissural axons in the embryonic spinal cord, Cell. 78 (3) (1994) 425–435.
[23] J.D. Lauderdale, N.M. Davis, J.Y. Kuwada, Axon Tracts Correlate with Netrin-1a Expression in the Zebrafish Embryo, Molecular and Cellular Neuroscience. 9 (1997) 293–313, https://doi.org/10.1006/mcne.1997.0624.
[24] R.D. Madison, A. Zomorodi, G.A. Robinson, Netrin-1 and Peripheral Nerve Regeneration in the Adult Rat, Experimental Neurology. 161 (2000) 563–570, https://doi.org/10.1006/exnr.1999.7292.
[25] I. Hernandez-Morato, S. Sharma, M.J. Pitman, Changes in neurotrophic factors of adult rat laryngeal muscles during nerve regeneration, Neuroscience. 333 (2016) 44–53, https://doi.org/10.1016/j.neuroscience.2016.07.004.
[26] K. Hong, L. Hinck, M. Nishiyama, M.M. Poo, M. Tessier-Lavigne, E. Stein, A ligand-gated association between cytoplasmic domains of UNC5 and DCC family receptors converts netrin-induced growth cone attraction to repulsion., Cell. 97 (1999) 927–41. 10.1016/s0092-8674(00)80804-1.
[27] L.I. Finci, N. Krüger, X. Sun, J. Zhang, M. Chegkazi, Y. Wu, G. Schenk, H.D. T. Mertens, D.I. Svergun, Y. Zhang, J. Wang, R. Meijers, The Crystal Structure of Netrin-1 in Complex with DCC Reveals the Bifunctionality of Netrin-1 As a Guidance Cue, Neuron. 83 (2014) 839–849, https://doi.org/10.1016/j.neuron.2014.07.010.
[28] A.K. Dillon, A.R. Jevince, L. Hinck, S.L. Ackerman, X. Lu, M. Tessier-Lavigne, Z. Kaprielian, UNC5C is required for spinal accessory motor neuron development, Molecular and Cellular Neuroscience. 35 (2007) 482–489, https://doi.org/10.1016/j.mcn.2007.04.011.
[29] L.Y. Chiang, K. Poole, B.E. Oliveira, N. Duarte, Y.A.B. Sierra, L. Bruckner-Tuderman, M. Koch, J. Hu, G.R. Lewin, Laminin-332 coordinates mechanotransduction and growth cone bifurcation in sensory neurons, Nature Neuroscience. 14 (2011) 993–1000, https://doi.org/10.1038/nn.2873.
[30] P.D. Yurchenco, W.G. Wadsworth, Assembly and tissue functions of early embryonic laminins and netrins, Current Opinion in Cell Biology. 16 (2004) 572–579, https://doi.org/10.1016/j.ceb.2004.07.013.
[31] S. Plantman, M. Patarroyo, K. Fried, A. Domogatskaya, K. Tryggvason, H. Hammarberg, S. Cullheim, Integrin-laminin interactions controlling neurite outgrowth from adult DRG neurons in vitro, Molecular and Cellular Neuroscience. 39 (2008) 50–62, https://doi.org/10.1016/j.mcn.2008.05.015.
[32] V.H. Höpker, D. Shewan, M. Tessier-Lavigne, M.M. Poo, C. Holt, Growth-cone attraction to netrin-1 is converted to repulsion by laminin-1, Nature. 401 (1999) 69–73, https://doi.org/10.1038/43441.
[33] R.W. Burgess, T.J. Jucius, S.L. Ackerman, Motor axon guidance of the mammalian trochlear and phrenic nerves: Dependence on the netrin receptor Unc5c and modifier loci, Journal of Neuroscience. 26 (2006) 5756–5766, https://doi.org/10.1523/JNEUROSCI.0736-06.2006.
[34] E.M. Ratcliffe, F. D'Autréaux, M.D. Gershon, Laminin terminates the netrin/DCC mediated attraction of vagal sensory axons, Developmental Neurobiology. 68 (2008) 960–971, https://doi.org/10.1002/dneu.20634.
[35] M.B. Montalbano, I. Hernández-Morato, L. Tian, V.X. Yu, S. Dodhia, J. Martinez, M. J. Pitman, Recurrent Laryngeal Nerve Reinnervation in Rats Posttransection: Neurotrophic Factor Expression over Time, Otolaryngology - Head and Neck Surgery (United States). 161 (2019) 111–117, https://doi.org/10.1177/0194599819831289.
[36] C.A. Schneider, W.S. Rasband, K.W. Eliceiri, NIH Image to ImageJ: 25 years of image analysis, Nature Methods. 9 (2012) 671–675, https://doi.org/10.1038/nmeth.2089.
[37] H. Mustafa, S. El Awdan, G. Hegazy, G. Abdel Jaleel, Prophylactic role of coenzyme Q10 and Cynara scolymus L on doxorubicin-induced toxicity in rats: Biochemical and immunohistochemical study, Indian Journal of Pharmacology. 47 (2015) 649–656, https://doi.org/10.4103/0253-7613.169588.
[38] L. Rieppo, L. Janssen, K. Rahunen, P. Lehenkari, M.A.J. Finnilä, S. Saarakkala, Histochemical quantification of collagen content in articular cartilage, PLoS ONE. 14 (2019), https://doi.org/10.1371/journal.pone.0224839.
[39] N. Tsanov, A. Samacoits, R. Chouaib, A.M. Traboulsi, T. Gostan, C. Weber, C. Zimmer, K. Zibara, T. Walter, M. Peter, E. Bertrand, F. Mueller, SmiFISH and FISH-quant - A flexible single RNA detection approach with super-resolution capability, Nucleic Acids Research. 44 (2016), https://doi.org/10.1093/nar/gkw784.
[40] RStudio Team, RStudio: Integrated Development for R. (2015).
[41] D. Sage, L. Donati, F. Soulez, D. Fortun, G. Schmit, A. Seitz, R. Guiet, C. Vonesch, M. Unser, DeconvolutionLab2: An open-source software for deconvolution microscopy, Methods. 115 (2017) 28–41, https://doi.org/10.1016/j.ymeth.2016.12.015.
[42] P. Virtanen, R. Gommers, T.E. Oliphant, et al., SciPy 1.0: fundamental algorithms for scientific computing in Python, Nature Methods. 17 (2020) 261–272, https://doi.org/10.1038/s41592-019-0686-2.
[43] I.F. Caplan, I. Hernandez-Morato, M.J. Pitman, Laminin-111 and Netrin-1: Supplementary Dataset, Mendeley Data. (2022), https://doi.org/10.17632/pjs7k4pfpx.2.
[44] J. Siironen, M. Sandberg, V. Vuorinen, M. Röyttä, Laminin B1 and Collagen Type IV Gene Expression in Transected Peripheral Nerve: Reinnervation Compared to Denervation, Journal of Neurochemistry. 59 (1992) 2184–2192, https://doi.org/10.1111/j.1471-4159.1992.tb10110.x.
[45] S.J. Armstrong, M. Wiberg, G. Terenghi, P.J. Kingham, Laminin activates NF-κB in Schwann cells to enhance neurite outgrowth, Neuroscience Letters. 439 (2008) 42–46, https://doi.org/10.1016/j.neulet.2008.04.091.
[46] X. Navarro, W.R. Kennedy, N.J. Stewart, L.T. Furcht, Effects of laminin on functional reinnervation of target organs by regenerating axons, Neuroreport. 2 (1991) 37–40, https://doi.org/10.1097/00001756-199101000-00009.
[47] X. Li, Netrin Signal transduction and the GEF Dock180 in attractive signaling, Nature Neuroscience. 11 (2008) 28–35.